

Stability of vacancies during solute clustering in Al-Cu-based alloys

A. Somoza,* M. P. Petkov,[†] and K. G. Lynn

Department of Physics, Washington State University, Pullman, Washington 99164-2814

A. Dupasquier[‡]

Istituto Nazionale di Fisica della Materia and Dipartimento di Fisica, Politecnico di Milano, Piazza L. da Vinci 32, 20133 Milano, Italy

(Received 10 August 2001; published 7 February 2002)

A direct comparison between Al-Cu and Al-Cu-Mg alloys shows that the mechanism, by which Mg affects the microstructure and the aging kinetics of the alloys, is related to the formation of vacancy-Cu-Mg complexes that act as embryos for the nucleation of coherent solute clusters. The presence of Mg stabilizes the vacancies in the Guinier-Preston (GP) zones. Experimental evidence of the association of the vacancies with the solute atoms was obtained by Doppler-broadening spectroscopy of the positron annihilation radiation using two Ge detectors in coincidence. The evolution of the average content of Cu in the proximity of the vacancies was monitored at different stages of aging at temperatures below the solvus of GP zones, after the solution heat treatment of the alloy.

DOI: 10.1103/PhysRevB.65.094107

PACS number(s): 78.70.Bj, 81.40.Cd

I. INTRODUCTION

The structural evolution of a metal alloy prepared in the form of a supersaturated solid solution (SSSS) is strongly influenced by the composition of the system and by the sequence of thermal treatments. Various kinds of lattice-coherent aggregates [solute-rich clusters, Guinier-Preston (GP) zones] and precipitates can be formed. The presence of a fine intragranular dispersion of these particles is beneficial for the mechanical qualities (hardness and strength) of the material, as it hinders the movement of dislocations under an applied stress. The technological importance of this phenomenon, referred to as *age hardening*, has stimulated an intense research effort since its discovery at the beginning of the last century.¹ Modern investigation is especially focused on the earliest decomposition stage (solute clustering and GP zone formation), as this is a crucial step for determining the final microstructure.

The full power of three-dimensional (3D) imaging techniques with atomic resolution has been recently applied to investigate the morphology of solute clusters in Al-based alloys.² These otherwise detailed pictures, however, contain no information on vacant lattice sites in the solute-rich clusters.³ Studies of vacancy kinetics unveil a new dimension in this field, as vacancies (V) play a key role in the transport of solute and the energetic stabilization of the cluster. These issues can be addressed by means of positron annihilation spectroscopy (PAS), which is specific for the detection of vacancies due to the propensity of thermalized positrons in a solid to become trapped in vacancylike defects.⁴ PAS has been applied to the study of Al alloy decomposition for more than 20 years, using lifetime spectroscopy (LS) or conventional Doppler-broadening (DB) analysis of the positron annihilation radiation.^{5,6} Recently, Somoza *et al.*⁷ used LS to address the decomposition kinetics of Al-Cu-based alloys with minority additions of Mg and Ag. The LS technique gives only indirect information on the chemical environment of the vacancies where the positrons are trapped. More specific data on the local chemical composition can be obtained

by coincidence Doppler-broadening (CDB) spectroscopy.⁸ The chemical sensitivity of this advanced variant of the DB technique has been discussed by Asoka-Kumar *et al.*⁹ CDB has been used for the recognition of impurity-defect complexes in semiconductors;¹⁰ the first applications to Al-based alloys have been published quite recently by Biasini *et al.*¹¹ and by Nagai *et al.*¹² A preliminary account of the present work has been presented by Somoza.¹³

In the present work, we address the mechanism by which Mg, a minority alloying element, affects the aging kinetics and the structure of the decomposition products in Al-Cu-based alloys. Experimental evidence from CDB and depth profiling with conventional DB is presented in a direct comparison between the Al-Cu and Al-Cu-Mg systems. We demonstrate that in the binary Al-Cu alloy a fraction of solute Cu atoms reacts with quenched-in vacancies forming V -Cu pairs, which mediate the formation of solute aggregates; these vacancies are progressively released as aging proceeds toward the formation of GP zones. In the ternary alloy, the presence of Mg not only enhances the Cu concentration in the environment of quenched-in vacancies, but also guarantees the stable inclusion of vacancies in the lattice-coherent solute aggregates formed by aging at moderate temperatures (below 70 °C).

II. EXPERIMENT

The samples were cut from rods of laboratory binary and ternary alloys, obtained by melting highly pure components. The composition of the samples was Al-4 wt % Cu (corresponding to Al-1.74 at. % Cu) and Al-4 wt % Cu-0.3 wt % Mg (corresponding to Al-1.74 at. % Cu-0.35 at. % Mg) alloys. The same materials were previously used for the LS measurements reported in Ref. 7. Well-annealed 99.9999% pure Al(100), 99.999% pure Cu(100) single crystals, and a polycrystalline Mg sample (purity >99.99%) were used to characterize the CDB response to defect-free metals; defect signatures, originating from the positron confinement, were observed with plastically deformed (thickness reduction

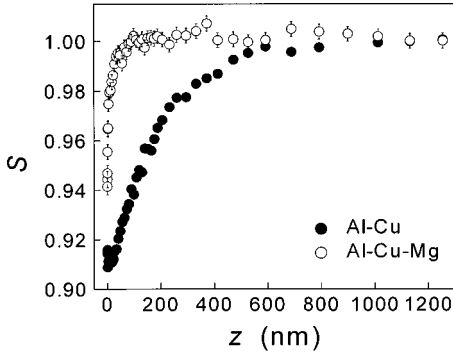


FIG. 1. S -parameter depth profile in Al-Cu (solid circles) and Al-Cu-Mg (open circles) after advanced aging below the solvus of GP zones (25 days/69 °C).

>50%) polycrystalline samples Al, Cu, and Mg of equivalent purity. The alloy samples were homogenized at 520 °C for 2 h, then quenched in an ice-water mixture (0 °C), which produced the SSSS (“as-quenched” state). After aging at the selected temperature (25 or 69 °C), the samples were stored in liquid N₂ between measurements. The measurements for the as-quenched sample were carried out at 17 K, while the temperature never exceeded 120 K during sample transition from air to vacuum; all other measurements were done at room temperature (RT) (~25 °C).

A variable energy (0–70 keV) positron beam with a rate of $\sim 2 \times 10^5 \text{ s}^{-1}$ was used for these experiments. Depth profiling by conventional DB was performed in the full energy range with a high-efficiency high-purity Ge (HPGe) detector, with an energy resolution of 1.45 keV at 514 keV (⁸⁵Sr). Spectra with 2×10^6 events were acquired at each positron energy. The depth profiles of the Doppler parameters S and W (Ref. 14) versus the beam energy were analyzed to extract the positron diffusion length [using VEPFIT (Ref. 15)], which sheds light on the positron trapping rate at vacancy-solute complexes. Short diffusion lengths (17–32 nm) were obtained for Al-Cu-Mg samples at all stages of aging, as well as for Al-Cu in the as-quenched state or aged at RT; however, after aging for 25 days at 69 °C, the diffusion length in Al-Cu was increased to $126 \pm 5 \text{ nm}$, not far from the value expected for defect-free Al (150–180 nm).¹⁶ A comparison between S profiles in aged Al-Cu and Al-Cu-Mg is shown in Fig. 1.

A second HPGe detector with similar characteristics was used for the coincidence CDB experiments. The combined energy resolution was 2.15 keV for the full Doppler shift. The beam energy was fixed to 60 keV, at which the positrons probe the bulk of the samples ($\sim 10 \mu\text{m}$ mean implantation depth). Timing coincidence was enforced, and the annihilation events were analyzed for conserved total energy: the sum of the deposited energies in the two detectors must equal the mass of the annihilation particles ($E_1 + E_2 = 2m_0c^2$) within an acceptance window of $\pm 2.5 \text{ keV}$. This requirement was used to filter the real annihilation events from the accidental coincidences.^{8,9} A peak-to-background greater than 10^5 was achieved, which ensured sensitivity to annihilation events with high-momentum (core) electrons. Two-dimensional spectra with $6\text{--}8 \times 10^7$ counts were collected, from which the virtually background-free Doppler spectra

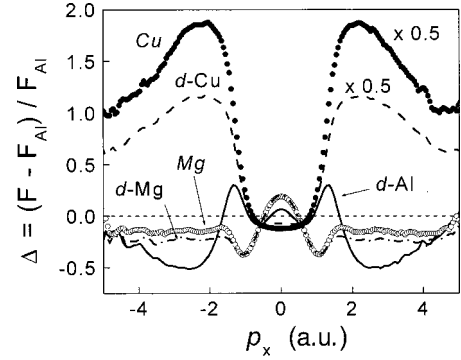


FIG. 2. CDB data for defect-free Cu (solid circles), defect-free Mg (open circles), deformed Al (d -Al, solid line), deformed Cu (d -Cu, dashed line), deformed Mg (d -Mg, dash-dotted line). The horizontal line at $\Delta = 0$ corresponds to the reference (defect-free Al).

were isolated and normalized to integral counts. These spectra (a function F of p_x , the momentum component of the annihilated e^+e^- pair along the photon propagation direction) were analyzed in terms of a ratio-difference parameter with respect to the spectrum F_{Al} obtained for well-annealed pure Al(100): $\Delta(p_x) = (F - F_{\text{Al}}) / F_{\text{Al}}$. The Δ values are presented below without smoothing or symmetrization for $|p_x| < 5 \text{ a.u.}$ (1 a.u. $\approx 7.3 \times 10^{-3} m_0c$), where the relevant information is contained.

III. RESULTS AND DISCUSSION

The CDB results for the reference samples (Fig. 2) provide the alphabet that one needs to read into the curves for the alloys. The Δ parameter for Cu(100) (solid circles in Fig. 2) shows a strong contribution from annihilation with fast electrons (3d and core), giving rise to the broad peaks at $\pm 2.1 \text{ a.u.}$ The shape of these “wings” is the “fingerprint” of the annihilation with Cu 3d and core electrons, which we use for evaluating the relative contribution of Cu to annihilation in an alloy. The depression ($\Delta < 0$) at low momenta is due to the smaller probability of annihilation with free electrons, as compared to Al. In contrast, Mg shows (open circles in Fig. 2) enhanced free-electron annihilation with respect to Al despite the identical ($1s^2 2s^2 2p^6$) core structure; positrons, confined to the interstitial regions of the less compact Mg lattice, have a smaller chance of interacting with core electrons. The features in the Δ parameter ($\pm 1\text{--}1.5 \text{ a.u.}$) originate from the different Fermi momenta of Mg (0.72 a.u.) and Al (0.93 a.u.),¹⁷ which result in sharp slope changes of the respective momentum distribution curves¹⁸ (the 3d electrons obscure this effect for Cu). The absence of structures in the high-momentum region of the Mg curve makes the direct detection of Mg in an Al matrix nearly impossible; indirect evidence is thus required to establish the Mg decoration of the vacancy-solute atom complexes in Al-Cu-Mg.

Positron localization at defects creates distinct features in the Δ parameter, more pronounced in materials with high Fermi energy, such as Al. These features are evident in the Δ curve of deformed (>50%) Al (solid line in Fig. 2), in which the majority of positrons annihilate in vacancy like defects

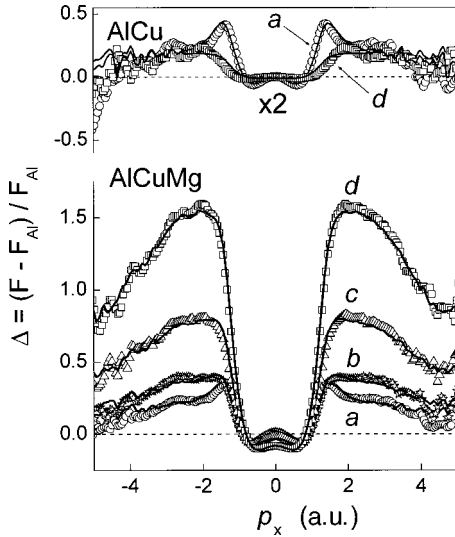


FIG. 3. CDB data for Al-Cu (top) and Al-Cu-Mg (bottom) at various stages of aging: (a) as-quenched (supersaturated solid solution), (b) initial aging (3.5 days/RT), (c) intermediate aging (25 days/RT), and (d) advanced aging (25 days/69 °C). The Al-Cu data are scaled by a factor of 2 for better readability. The solid lines are the result of a linear fitting (see text).

(e.g., dislocation jogs). The positron confinement at a missing ion site leads to enhanced annihilation with free electrons (giving $\Delta > 0$ at 0 a.u.), at the expense of the annihilation with core electrons (suppressed Δ values in the ± 2 –5 a.u. regions). The two peaks at ± 1.3 a.u. arise from the smearing of the momentum distribution around the Fermi momentum due to the spatially confined positron wave function. Note that the momentum values at which these features appear are unique; however, their relative intensity depends on the experimental conditions (detector resolution, degree of deformation, sample quality, etc.; for a comparison, see Lynn *et al.*¹⁹). Positron annihilation with low-momentum electrons is also enhanced by trapping in deformed Al and Mg samples (Fig. 2, dashed and dash-dotted lines, respectively). The Cu signature, still easily identifiable ($|p_x| > 2$ a.u.), stands at roughly 2/3 of that measured in Cu(100).

Figure 3 depicts the Δ profiles for the Al-Cu (top) and Al-Cu-Mg (bottom) systems. The curves are labeled in order of the alloy evolution chronology: *a* denotes SSSS (as-quenched samples), *b* (shown only for Al-Cu-Mg) initial aging (3.5 days at RT), *c* (shown only for Al-Cu-Mg) intermediate aging (25 days at RT), and *d* advanced aging (25 days at 69 °C). The solid lines are the result of a linear fitting to be explained below. For the as-quenched samples of both alloys, the profiles (curves *a*) contain a clear localization signature (central relative maximum and peaks at ± 1.3 a.u.) as well as the Cu fingerprint (wings at $|p_x| > 2$ a.u.). The localization signal, combined with the Cu signature, indicates the presence of quenched-in vacancies, possibly forming V-solute complexes containing Cu. Surprisingly, the intensity of the Cu signature is almost double for the ternary alloy than for the binary alloy. This shows that the presence of Mg as a minority alloying element enhances the presence of Cu at the annihilation site; the high Cu/Mg ratio of the

present alloy is probably an important factor, since CDB data taken for Al–1.1 at. % Cu–1.7 at. % Mg (Ref. 12) compared to Al-Cu show suppression rather than enhancement of the Cu signal. When aging proceeds (curves *b*–*d*), Al-Cu and Al-Cu-Mg display opposite behaviors. For the binary system, the signature of positron confinement becomes progressively weaker and finally disappears; the signature of Cu also decreases, although a weak signal persists even at the most advanced stage of aging. For the ternary alloy, not only the signal of vacancylike defects persists, but the Cu signature becomes progressively stronger. The same trends have been observed for Al–1.7 at. % Cu and Al–1.7 at. % Cu–1.3 at. % Mg aged at 150 °C by Nagai *et al.*¹²

For a more quantitative appraisal of the results described above, we have fitted the experimental data of Fig. 3 with linear combinations of the momentum distributions obtained for the alloy components, as given by the equation

$$F_{\text{alloy}} = w_{\text{Al}} F_{\text{Al}} + w_{\text{Al}^*} F_{\text{Al}^*} + w_{\text{Mg}^*} F_{\text{Mg}^*} + w_{\text{Cu}^*} F_{\text{Cu}^*}, \quad (1)$$

where the weights of the linear combination obey the normalization condition

$$w_{\text{Al}} + w_{\text{Al}^*} + w_{\text{Mg}^*} + w_{\text{Cu}^*} = 1 \quad (2)$$

($w_{\text{Mg}^*} = 0$ in the case of Al-Cu). In the above equations, the subscripts Al*, Mg*, and Cu* refer to data obtained for the cold-worked samples, which are included in the linear combination to mimic the effects of the positron confinement. Least-squares adjustment in the interval $|p_x| \leq 4$ a.u. gives the solid lines shown in Fig. 3. The corresponding weights are reported in Table I, together with the average positron lifetimes taken from Ref. 7.

It is worth discussing the physical meaning of the w coefficients. The ratios of the first three coefficients (w_{Al} , w_{Al^*} , and w_{Mg^*}) are essentially determined by structures in the low-momentum region, where the elemental specificity of CDB data in the alloy is lost. Therefore the assignment of a distinct meaning to these coefficients is questionable in principle. Although the weight of the deformed-Al component (w_{Al^*}), determined by the confinement signal near to the Fermi break is a good qualitative indicator of positron trapping in vacancylike defects, it cannot be taken as a measure of the fraction of positrons annihilated at vacancies, since the geometry and chemistry of a decorated trap in the alloy are not the same as in the deformed-Al reference. For the same reason, w_{Al} is not a measure of the positron fraction annihilating in bulk Al; indeed, the lifetime measurements⁷ and the diffusion length measurements show strong trapping (trapped fraction near to 100%) in all cases excepted aged Al-Cu. In the case of the Mg component, not only the absence of high-momentum structures, but also the difficulty of the numerical separation from the similar Al component (the accuracy of the w_{Mg^*} coefficient is 20% or worse) does not warrant a quantitative determination of the Mg signal from CDB data. Thus we prefer to be more conservative than Nagai *et al.*¹² and limit ourselves to observe that the small values of w_{Mg^*} reported in Table I are qualitatively consistent with the small percentage of Mg contained in the alloy.

TABLE I. Weights of the linear combination fitting of CDB data for Al-Cu and Al-Cu-Mg at different stages of aging. Absolute statistical errors of the order of 0.02 for w_{Al} , w_{Al^*} , and w_{Mg^*} , of the order of 0.01 for the sum of these coefficients as well as for w_{Cu^*} . Average positron lifetimes after Somoza *et al.* (Ref. 7).

Alloy	Aging	w_{Al}	w_{Al^*}	w_{Mg^*}	w_{Cu^*}	τ_{av} (ps)
Al-Cu	No aging	0.71	0.20		0.09	204 ± 0.5
Al-Cu	25 days/RT	0.89	0.05		0.06	169 ± 0.5
Al-Cu	25 days/69 °C	0.96	0.00		0.04	161 ± 0.5
Al-Cu-Mg	No aging	0.53	0.27	0.04	0.16	212 ± 0.5
Al-Cu-Mg	3.5 days/RT	0.55	0.15	0.10	0.20	197 ± 0.5
Al-Cu-Mg	25 days/RT	0.43	0.15	0.05	0.37	194 ± 0.5
Al-Cu-Mg	25 days/69 °C	0.15	0.12	0.04	0.69	184 ± 0.5

The situation, however, is different with Cu: the “finger-print” at high momentum is easily identifiable and its nearly atomic character ensures that its shape is almost the same in a pure Cu reference and in the alloy. Therefore, w_{Cu^*} can safely be considered proportional to the positron overlap probability with Cu cores. The coefficient of proportionality depends on the arbitrary choice of the reference (for instance, taking as a reference well-annealed Cu instead of deformed Cu would decrease the weight of the Cu component by about 2/3). Thus to stay on the safe side, the physical meaning of w_{Cu^*} variations should be discussed only in relative terms. The positron overlap with Cu is an information less interesting from the point of view of the knowledge of the microstructure of the material than the Cu concentration at the defects where the positron annihilates. However, relating these two parameters is not a trivial problem, since the positron contact with the atomic cores depends on the local atomic geometry and on the affinity of the positron to the different atoms. To solve this problem, sophisticated model calculations are required.

Below, we adopt a simpler approach with smaller but sufficient accuracy to derive quantitative information from the Cu signature. We have chosen deformed Cu as a reference for the Cu high-momentum signal, in which situation nearly all positrons are trapped in open volume defects. Thus the reduction of the positron overlap to Cu due to localization into a vacancylike defect is accounted for in an approximated way since the beginning. Therefore, in all cases of saturated trapping (as occurs in all cases, excepted aged Al-Cu), the w_{Cu^*} coefficients of Table I are can be taken as an approximated measurement of the local Cu concentration at the annihilation site. Of course, this approximation must be taken with caution, as it neglects the changes of the positron overlap with atomic cores occurring when passing from traps in pure Cu to Cu-decorated traps in the alloy.

Support for this simplified approach comes from the calculation of the w_{Cu^*} coefficient for as-quenched Al-Cu, $w_{\text{Cu}^*} = 0.09 \pm 0.01$ (Table I), which corresponds to one Cu atom per vacancy ($1/12 \approx 0.083$) within the experimental error. Since vacancies in Al are mobile at RT, they can survive quenching only if stabilized in a complex with foreign atoms, which in this sample is Cu. This finding is opposite to the conclusion proposed by Nagai *et al.*,¹² despite reported similarity to our experimental data. The origin of this discrepancy is in their use of crystalline Cu spectrum as a ref-

erence, which leads to an underestimation of the average Cu signal from the decorated vacancies in Al-Cu and thereby suggesting the existence of undecorated Al vacancies.

Passing from as-quenched Al-Cu to as-quenched Al-Cu-Mg, the value of w_{Cu^*} increases from 0.09 to 0.16. Following the same line of interpretation proposed above, this result can be taken as the signal of vacancy-solute complexes containing on the average about two Cu atoms per vacancy. Although the presence of Mg together with Cu in the same solute-vacancy cluster cannot be directly inferred from the linear fit coefficients for the reasons explained above, fast aggregation of Cu to V-Mg pairs seems the only possible explanation for the different behavior of Al-Cu-Mg and of Al-Cu displayed in Fig. 3. We are aware that this interpretation is difficult to reconcile with the absence of Cu-Mg co-clusters in the same alloy reported by Ringer *et al.*²⁰ on the basis of atom probe (AP) scans, unless one admits that only a fraction of Mg atoms, too small to be detected by AP, forms vacancy-solute complexes. In this connection, note that the lower limit of sensitivity of all positron techniques to vacancylike defects in Al is of the order of 1 at. ppm, about two order of magnitude below the lower concentration limits of typical AP experiments (about 2×10^4 atoms are collected in the AP scans of Ref. 20).

The Cu enrichment of the vacancy-solute clusters, as monitored by the increase of the w_{Cu^*} coefficient, proceeds with aging. After 25 days at 69 °C, the signal is more than 4 times bigger than in the as-quenched state, about 8 times than in as-quenched Al-Cu. It may be inferred from this datum that average environment seen by the positron at the annihilation site in these conditions is 60%–70% Cu, as expected for about 8 Cu atoms over the 12 nearest-neighbor sites of a vacancy in a fcc lattice. This information deserves a comment. Normally, CDB data, as well as PAS results in general, give information on the local structure of the trap, but have no direct sensitivity to the structure of the material far from the annihilation site. Therefore PAS experiments that show positron trapping at vacancies in an alloy in most cases cannot tell anything about the size and shape of the structural or chemical inhomogeneity associated with a vacancy. For instance, by PAS alone it is difficult to tell whether a trapping center is contained in a GP zone or in a structureless cluster. The present case, however, is a partial exception to this rule, as it can be concluded that the Cu-rich structures seen by positrons in aged Al-Cu-Mg are three-

dimensional objects: a cluster or a stack of Cu layers intercalated by a single Al plane. Indeed, vacancies contained in Cu monolayers or in multilayers with two or more Al intercalated planes cannot accommodate the high Cu fraction at the annihilation site revealed by the present CDB results. Of course, this is not a proof of the nonexistence of GP zones in the form of monolayers or doubly intercalated multilayers, which are often observed by high-resolution electron microscopy in Al-Cu and Al-Cu-Mg alloys,^{21,22} but tells that these structures do not contain the vacancies that are necessary to trap the positrons. Most probably, Mg is a minority component of the three-dimensional structure, where it stabilizes the vacancy. This statement is supported by the comparison with Al-Cu at the same aging, where only a weak Cu signal ($w_{\text{Cu}^*}=0.04$) survives and there are no symptoms of positron trapping (lifetime close to bulk Al,⁷ long diffusion length, $w_{\text{Al}^*}=0$). The residual Cu signal in aged Al-Cu (note, however, that in this case w_{Cu^*} is not a good approximation to the concentration) would then result from the enhancement, without trapping, of the positron wavefunction within GP zones, which is due to the larger affinity of positrons for Cu than for Al.²³

IV. CONCLUSIONS

The findings of the present work can be summarized as follows.

(a) In Al-Cu, V-Cu pairs are present immediately after quenching. The vacancies are gradually released when aging progresses with the formation of Cu clusters or GP zones. Positrons are attracted by these aggregations of solute, but

are not deeply trapped. This conclusion, which comes from fully consistent measurements of positron lifetime,⁷ diffusion length and CDB spectra, supports the so-called pump model of solute aggregation (when a mobile V-Cu pair gets to a cluster, the vacancy is released and can react again with isolated Cu atoms to form a new V-Cu pair²⁴).

(b) In Al-Cu-Mg, the Cu concentration at the positron annihilation site immediately after quenching is higher than in Al-Cu. Aging leads to a further increase of the Cu local concentration. Starting from about 16% after quenching, the Cu concentration at the positron trap becomes so high (almost 70% after 25 days at 69 °C) that implies the existence of three-dimensional Cu-rich structures. The result is consistent with the progressive increase of the Cu concentration at the vacancy, proposed by Somoza *et al.*⁷ for interpreting the positron lifetime decrease observed in this alloy upon aging. Apparently, the initial V-Cu-Mg complexes act as embryos for further aggregation of Cu; Monte Carlo simulations also indicate a mechanism of nucleation of Cu onto V-Mg complexes.²⁵ Since the vacancies are not released, the transport of Cu must be mediated by formation of new V-Cu pairs with thermal equilibrium vacancies. The activation energy controlling the progress of decomposition is then increased to 0.65 eV, in comparison to 0.32 eV in Al-Cu.⁷

(c) Detection of immediate formation of solute-vacancy clusters upon quenching, followed by further aggregation of Cu onto V-Mg seeds, is in accordance with the dependence of the as-quenched hardness values on the Mg content²⁴ and with calorimetric evidence of rapid solute aggregation in Al-Cu-Mg alloys.²⁶

*Permanent address: IFIMAT Universidad Nacional del Centro de la Provincia de Buenos Aires and Comisión de Investigaciones Científicas de la Provincia de Buenos Aires Pinto 399, B7000GHG Tandil, Argentina.

†Permanent address: Jet Propulsion Laboratory, California Institute of Technology, 4800 Oak Grove Dr., Pasadena, CA 91109.

‡Corresponding author.

Electronic address: alfredo.dupasquier @fisi.polimi.it

¹A. Wilm, *Metallurgie (Halle)* **8**, 22 (1911).

²K. Hono, *Acta Mater.* **47**, 3127 (1999).

³I. J. Polmear, in *Proceedings of the 12th International Conference on Positron Annihilation*, München, Germany, 2000, edited by W. Triftshäuser, G. Kögel, and P. Sperr [*Mater. Sci. Forum* **363-365**, 1 (2001)].

⁴P. Hautojärvi and C. Corbel, in *Positron Annihilation Spectroscopy*, edited by A. Dupasquier and A. P. Mills (IOS, Amsterdam 1993), p. 491.

⁵R. Krause, G. Dlubek, and O. Brümmer, in *Proceedings of the European Meeting on Positron Studies of Defects*, edited by G. Dlubek, O. Brümmer, G. Brauer, and K. Hennig (Martin Luther University, Halle, 1987), p. 7.

⁶A. Dupasquier, P. Folegati, N. de Diego, and A. Somoza, *J. Phys.: Condens. Matter* **10**, 10409 (1998).

⁷A. Somoza, R. Ferragut, A. Dupasquier, P. Folegati, and I. J. Polmear, *Phys. Rev. B* **61**, 14454 (2000); **61**, 14464 (2000).

⁸J. R. MacDonald, K. G. Lynn, R. A. Boie, and M. F. Robbins,

Nucl. Instrum. Methods **153**, 189 (1978).

⁹P. Asoka-Kumar, M. Alatalo, V. J. Ghosh, A. C. Kruseman, B. Nielsen, and K. G. Lynn, *Phys. Rev. Lett.* **77**, 2097 (1996).

¹⁰M. P. Petkov, M. H. Weber, K. G. Lynn, R. S. Crandall, and V. J. Gosh, *Phys. Rev. Lett.* **82**, 3819 (1999).

¹¹M. Biasini, G. Ferro, P. Folegati, and G. Riontino, *Phys. Rev. B* **63**, 092202 (2001).

¹²Y. Nagai, M. Murayama, Z. Tang, T. Nonaka, K. Hono, and M. Hasegawa, *Acta Mater.* **49**, 913 (2001).

¹³A. Somoza, in *Proceedings of the 12th International Conference Positron Annihilation*, München, Germany, 2000, edited by W. Triftshäuser, G. Kögel, and P. Sperr [*Mater. Sci. Forum* **363-365**, 9 (2001)].

¹⁴P. J. Schultz and K. G. Lynn, *Rev. Mod. Phys.* **60**, 701 (1988).

¹⁵A. van Veen, H. Schut, J. de Vries, R. A. Hakvoort, and M. R. Ijpma, in *Positron Beams for Solids and Surfaces*, edited by P. J. Schultz, G. R. Massoumi, and P. J. Simpson, AIP Conf. Proc. No. 218 (AIP, New York, 1990), p. 171.

¹⁶E. Soininen, H. Huomo, P. A. Huttunen, J. Makinen, A. Vehanen, and P. Hautojärvi, *Phys. Rev. B* **41**, 6227 (1990).

¹⁷N. W. Ashcroft and N. D. Mermin, *Solid State Physics* (Saunders College, Philadelphia, 1976), p. 38.

¹⁸P. E. Mijnders, A. C. Kruseman, A. van Veen, V. J. Ghosh, P. Asoka-Kumar, A. Bansil, S. Kaprzyk, and K. G. Lynn, *Mater. Sci. Forum* **255-257**, 784 (1997).

¹⁹K. G. Lynn, J. E. Dickman, W. L. Brown, M. F. Robbins, and E.

- Bonderup, Phys. Rev. B **20**, 3566 (1979).
- ²⁰S. P. Ringer, K. Hono, I. J. Polmear, and T. Sakurai, Acta Mater. **44**, 1883 (1996).
- ²¹H. Fujita and C. Lu, Mater. Trans., JIM **33**, 892 (1992).
- ²²A. Charai, T. Walther, C. Alfonso, A.-M. Zahra, and C. Y. Zahra, Acta Mater. **48**, 2751 (2000).
- ²³M. J. Puska, P. Lanki, and R. M. Nieminen, J. Phys.: Condens. Matter **1**, 6081 (1989).
- ²⁴J. T. Vietz and I. J. Polmear, J. Inst. Met. **94**, 410 (1966).
- ²⁵S. Hirose, T. Sato, A. Kamio, and H. M. Flower, Acta Mater. **48**, 1797 (2000).
- ²⁶C. Y. Zahra, C. Alfonso, and A. Charai, Scr. Mater. **39**, 1553 (1998).